INVESTIGATION OF SPATIAL VARIATION OF THE SURFACE RESISTANCE OF A SUPERCONDUCTING RF CAVITY*

D. Gonnella, R. French, and M. Liepe, CLASSE, Cornell University, Ithaca, NY 14853

Abstract

Cornell has recently completed a 1.3 GHz single cell temperature mapping system with a resolution of a few tenths of a millikelvin, corresponding to a surface resistance resolution of 1 nOhm. A superconducting RF cavity was tested using temperature mapping and the surface resistance was extracted from the temperature mapping data as a function of position on the cavity surface. The surface resistance was profiled across the surface of the cavity between 5 and 30 MV/m and at different temperatures between 1.6 and 2.1 K. From BCS fitting of the local surface resistance, the spatial variation and the field dependence of the mean free path, energy gap, and residual resistance was found. These studies give interesting new insights into the degree of variation of the properties of the superconductor over the surface of the cavity.

INTRODUCTION

Superconducting RF cavities are the main driving force for modern particle accelerators and light sources. Under standing the fundamental properties of these cavities is cru cial to producing cavities with consistently high Q's an capable of achieving high accelerating gradients. The ma terial properties such as residual resistance, mean free path and energy gap can be extracted from experimentally ob tained data. The performance of cavities can be correlate with material properties to help produce better cavities. I this paper we discuss an ongoing effort at Cornell to ma out material properties of a cavity not only as a function c accelerating field but as a function of space.

CAVITY PREPARATION AND TESTING

A single-cell ILC shaped cavity was fabricated from fine grain niobium with a RRR of 300 by Niowave. It was prepared with bulk EP, 800°C bake, and 120°C bake and tested. Q_0 vs T, Q_0 vs E at various temperatures between 1.6 and 4.2 K, and resonance frequency vs temperature were measured. The cavity reached an accelerating field of 43 MV/m with a maximum Q_0 of 7.5×10^{10} at 8 MV/m. The full Q_0 vs E curve at 1.6 K is shown in Fig. 1.

The temperature mapping system developed at Cornell has a sensitivity on the order of a few tenths of a millikelvin. The T-map is organized into 38 boards, each with 17 resistors. The boards are placed azimuthally around the cavity, giving a full temperature profile of the cavity under operation. The heating at 30 MV/m and 1.6 K is shown in Fig. 2. Similar T-maps were taken at 5 MV/m intervals between 5 and 30 MV/m at 1.6, 1.8, 2.0, and 2.1 K. Heating

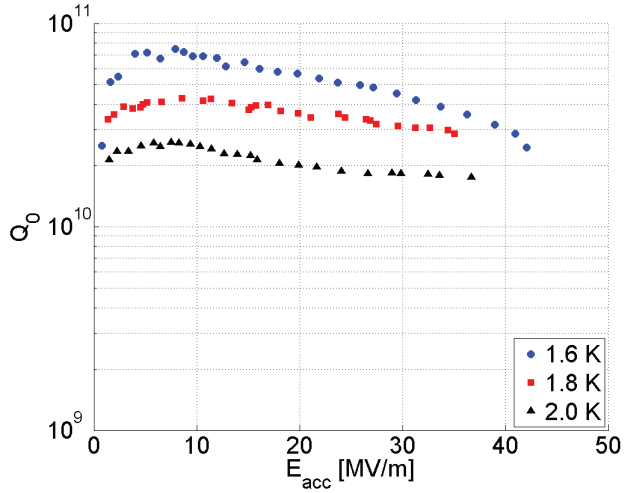

Figure 1: Q_0 vs E at 1.6, 1.8, and 2.0 K. Error bars are 10% on E and 20% on Q_0.

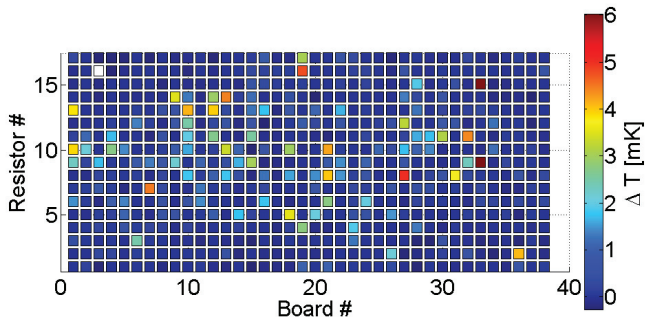

Figure 2: Heating at 30 MV/m and 1.6 K across the cavity. Resistor 9 is centered on the equator.

was very small, with a maximum of 6 mK in a few isolated spots, so thermal feedback effects do not have to be considered here.

BULK MATERIAL PROPERTIES

The material properties of the RF penetration layer can be extracted from the the resonance frequency vs temperature and Q_0 vs temperature data measured. This is done using SRIMP for BCS fitting [1] and the method described in [2]. The fit for change in penetration depth vs temperature (obtained from change in resonance frequency) is shown in Fig. 3. The fit for R_S vs temperature (obtained from Q_0) is shown in Fig. 4. The material properties extracted from the fits are shown in table 1, column 2. Note that these values

* Work supported by DOE Grant DE-SC0002329

ISBN 978-3-95450-143-4

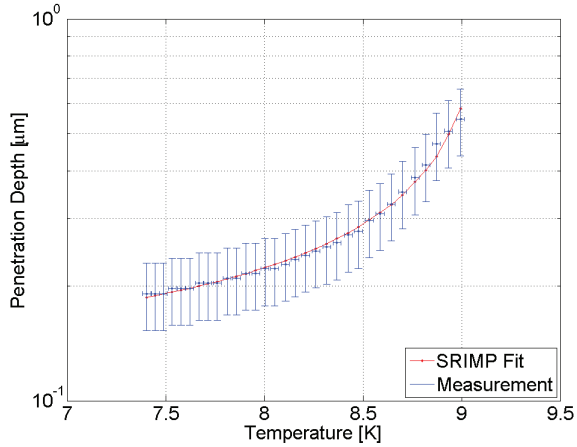

Figure 3: Fit of the penetration depth vs temperature using SRIMP to extract T_C and mean free path.

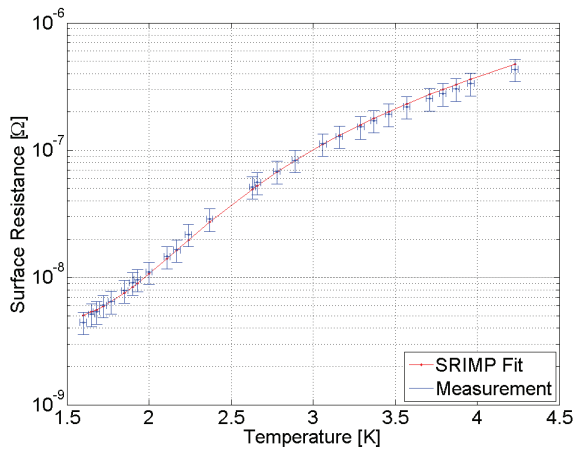

Figure 4: Fit of the surface resistance vs temperature using SRIMP to extract residual resistance and energy gap using the values obtained from Fig. 3 for T_C and mean free path.

are the average values of the RF surface layer of the cavity wall (extracted from data at low fields).

Using the Q_0 vs E data between 1.6 and 2.1 K, residual resistance and energy gap can be extracted from BCS fits as a function of accelerating field. The residual resistance vs field is shown in Fig. 5 and the energy gap vs field is shown in Fig. 6. The material properties at 30 MV/m are also shown in table 1, column 3. The low field Q_0 increase up to 10 MV/m is caused by a decreasing residual resistance. As shown in Fig. 6, the observed field dependence of the BCS surface resistance (see medium field Q slope at 2.0 K, see Fig. 1) can be well described by a field dependent energy gap. At 35 MV/m (150 mT peak surface magnetic field) the gap is reduced by about 10% relative to the low field value. Such a closing of the energy gap has been predicted for strong type-II superconductors [3].

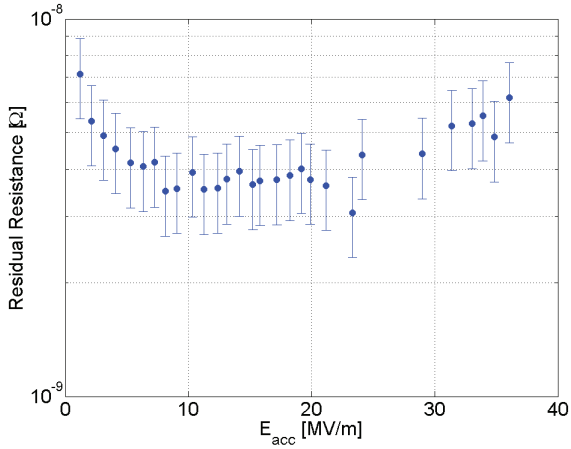

Figure 5: Residual resistance vs accelerating field.

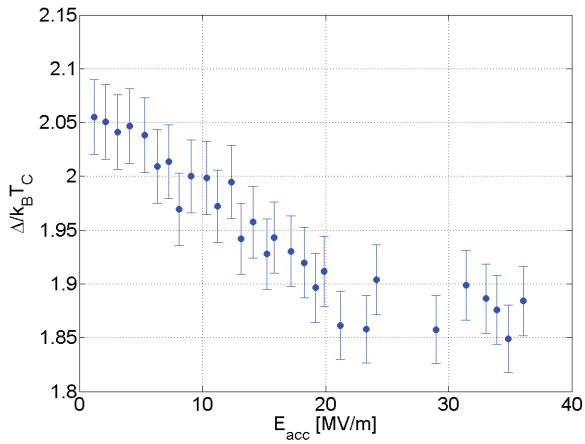

Figure 6: Energy gap vs accelerating field.

SPATIAL DISTRIBUTION OF MATERIAL PROPERTIES

The heating measured by each temperature sensor at each field point and each temperature was used in conjunction with a 1-dimensional heat conduction model to find the true temperature increase on the inside of the cavity wall at the location of the temperature sensors. Only signals that were above the noise floor were used to ensure accurate data. This heating was converted into surface resistance, and used to extract via BCS fits energy gap (Δ/k_BT_C), mean free path, and residual resistance. The spread of surface resistance vs temperature at each T-map point is shown in Fig. 7, in addition to the average surface resistance calculated from the measured Q values. Histograms at 30 MV/m of residual resistance, energy gap, and mean free path are shown in Fig. 8. The averages of these distributions are listed in the fourth column of table 1. The averages obtained are consistent with the values obtained from Fig. 3 and Fig. 4. It is clear from Fig. 8 that each of the BCS properties extracted show a spread centered around the average value obtained for the cavity from surface re-

Table 1: Summary of Extracted Material Properties

Property	Average Value of RF Penetration Layer at Low Fields	Average Value of RF Penetration Layer at 30 MV/m	Average from Spatial Distribution at 30 MV/m
T_c [K]	9.2 ± 0.9	9.2 (fixed)	9.2 (fixed)
$\Delta/k_B T_C$	1.96 ± 0.03	1.85 ± 0.03	1.85
Mean Free Path [nm]	23.5 ± 0.7	23.5 ± 0.7	26.3
R_{res} [nΩ]	4.3 ± 0.9	4.4 ± 0.9	4.3

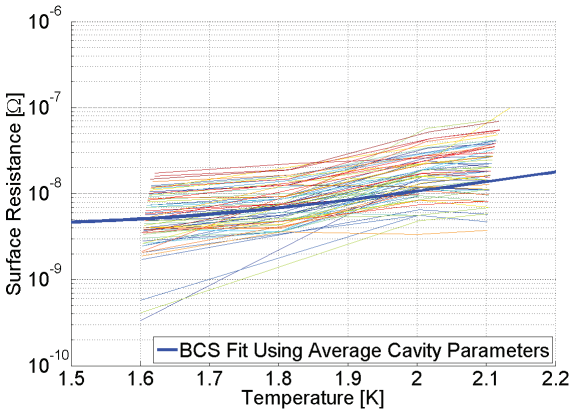

Figure 7: Surface resistance vs temperature at 30 MV/m for each usable resistor on the T-Map. Also shown is the temperature dependence of the average surface resistance determined from the measured low field quality factors.

sistance vs temperature. Spatially, the residual resistance varies up to a maximum of 15 $n\Omega$, the energy gap varies between 1.6 and 2.2, and the mean free path varies between about 15 and 40 nm.

Correlations between heating at 1.6 K and material properties extracted from the BCS fits were found. Fig. 9 shows residual resistance, energy gap, and mean free path at a given surface location plotted against its respective heating at 1.6 K and 30 MV/m. A linear fit is also shown. In each case, residual resistance and mean free path were found to increase with increasing heating. Energy gap was found to decrease with increasing heating. The is indicative of the gap closing with higher field as discussed in [3].

CONCLUSION

A single-cell ILC shaped cavity was tested with temperature mapping at various temperatures between 1.6 and 2.1 K. The resulting T-maps were used to calculate a surface resistance profile of the cavity at each temperature and field and used to extract material properties as a function of field and space. The resulting distributions were consistent with average material properties obtained from BCS fitting of resonance frequency vs temperature and Q_0 vs temperature. The mean free path and residual resistance were found to be increased for higher heating areas on the surface of the cavity. The energy gap was found to decrease with field

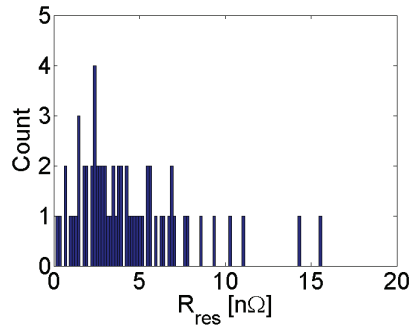

(a) Residual Resistance

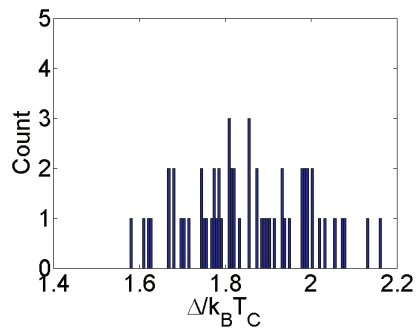

(b) Energy Gap ($\Delta/k_B T_C$)

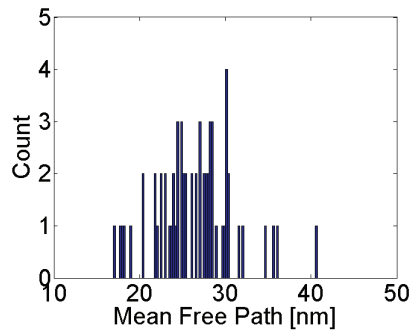

(c) Mean Free Path

Figure 8: Histograms of residual resistance, energy gap, and mean free path at 30 MV/m obtained from SRIMP fitting at each T-Map sensor location above the noise floor.

and with higher heating. This might be an observation of a theoretically predicted calculated previously showing the gap closes with increasing field.

Future work will involve improving the temperature mapping system. We will focus on repairing broken re-

ISBN 978-3-95450-143-4

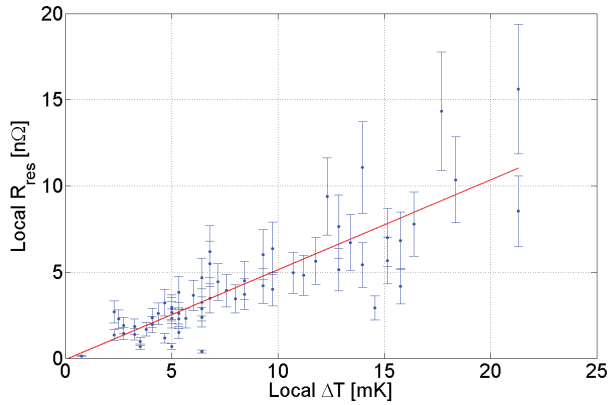

(a) Residual Resistance

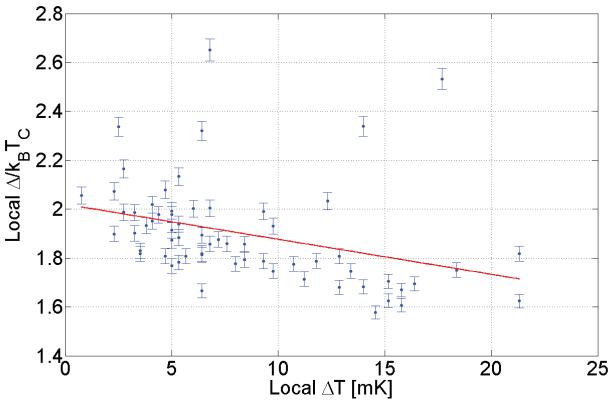

(b) Energy Gap ($\Delta/k_B T_C$)

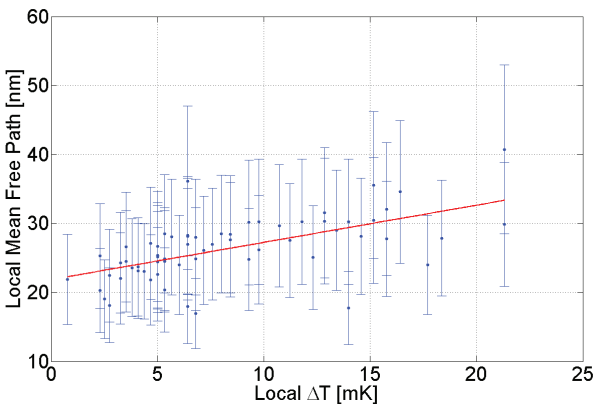

(c) Mean Free Path

Figure 9: Plots of material properties vs their corresponding heating at 1.6 K and 30 MV/m.

sistors to get a more complete profile of the cavity. Additionally, we will improve the temperature stability of the helium bath in order to lower the noise floor of the T-maps. With improved T-map, we will be able to obtain a full profile of residual resistance, mean free path, and energy gap for the cavity. The data and methods described here will be very useful in future studies of SRF cavities.

ACKNOWLEDGMENTS

The authors would like to thank Sam Posen, Daniel Hall, and Fiona Wohlfarth for assistance during cavity assembly and testing and Nicholas Valles for useful discussions about SRIMP. We would also like to thank the CLASSE support staff for assistance during chemistry and cavity preparation especially Brendan Elmore.

REFERENCES

[1] J. Halbritter, "FORTRAN-Program for the Computation of the Surface Impedance of Superconductors." KAROLA Externer Bericht 3/70-6 (1970).

[2] Dan Gonnella and Matthias Liepe, "High Q0 Studies at Cornell," Proceedings of the 16th International Conference on RF Superconductivity, Paris, FR (2013).

[3] Sam Posen and Matthias Liepe, "The Closing Quasiparticle Spectral Gap and its Implications for Nb3Sn," Presented at the 7th SRF Materials Workshop (2012).